*Acta of Bioengineering and Biomechanics*
*Vol. 9, No. 1, 207*

# Generation of a finite element model of the thoracolumbar spine

M.A. TYNDYK[a, b,*], V. BARRON[a], P.E. MCHUGH[a, b], D. O'MAHONEY[a]

[a] National Centre for Biomedical Engineering Science, National University of Ireland, Galway, Ireland
[b] Department of Mechanical and Biomedical Engineering, National University of Ireland, Galway, Ireland,
magdalena.tyndyk@nuigalway.ie; peter.mchugh@nuigalway.ie, valerie.barron@nuigalway.ie; denis.omahoney@nuigalway.ie;
Dr. Valerie Barron, National Centre for Biomedical Engineering Science, National University of Ireland, Galway, Ireland.
E-mail: valerie.barron@nuigalway.ie. Tel: +353 (0)91 524411 ex 2805. Fax: + 353 (0)91 750596

The goal of this study was to generate a realistic 3D FE model of the seven level thoracolumbar spine. This research focused on the development of a robust and efficient procedure for generating anatomical 3D FE models, directly from a series of medical images, i.e., CT data. A complex model of the spine was created by combining two different modelling approaches, namely the CAD and STL-CAD methods. In addition, the entire meshing procedure for the vertebrae was significantly speeded up by combining 3D tetrahedral elements with brick elements, relative to conventional mapped mesh generation procedures. The resulting model generation method allowed for flexibility in element choice and in element type combinations. The model was subjected to various compressive loads to asses the overall behaviour of the spine. This case study was performed to illustrate the usefulness of the FE model. In the authors' opinion, the model presented is an important tool in computational spine research as it can provide general information on spinal behaviour under various loading conditions whether healthy, diseased or damaged.

*Keywords: thoracolumbar spine, CAD, stereolithography (STL), FE*

## 1. Introduction

The human spine is a complex structure whose principal functions are to protect the spinal cord and transfer loads from the head and trunk to the pelvis. In recent years, computational modelling, especially Finite Element Analysis (FEA) has made an important contribution to the study and understanding of the behaviour of the spine. This method seems to be the most suitable approach to study spinal biomechanics due to the 3D irregular geometry, non-homogenous material arrangement, large complex loading and movement, and non-linear response including contact at facet joints [1]. As computing power and software capabilities have increased over the years, more complex models and spinal problems can be analysed and investigated. According to FAGAN et al. [2], FEA has been used in spine research for a number of reasons: (i) to examine biomechanical behaviour of the healthy spine, (ii) to assess the spinal performance when affected by disease, degenerative changes, trauma, ageing or surgery, (iii) to investigate the influence of various spinal instrumentation on spine behaviour, and (iiii) to assist in the design and development of new spinal implants.

Various FE models of the spine, especially the lumbar spine, have been proposed and reported in the literature in recent years. This is understandable given the prevalence of low back pain. In order to examine the effects of material property variation for the different spinal components, both simple and complex FE models of single vertebrae [3], [4], motion segments [5], [6], multimotion segments [7], [8] and the whole lumbar spine [9]–[11] have been proposed. However, similar investigations for the ex-

* Corresponding author.

tended thoracolumbar region have been rarely reported [12].

To date, the motion segment, consisting of two vertebrae and the disc that separates them, is a basic unit of study in spinal kinematics and commonly used in computational spinal research. However, in the authors' opinion multisegmental FE models of the spine have advantages over short "specimens" and can contribute more significantly to quantitative spinal biomechanical investigations. These models give more information on the condition and performance of the spine under different loading conditions. Moreover, they allow for the study of the load transfer mechanisms along the spine, and for the determination of the stress and strain distributions in the spinal column. The regions of the spine that are more susceptible to injury can be identified as the intersegmental results can vary for different motion segments. In addition to this, the general kinematics of the healthy spine can be examined, and the effect of various diseases (osteoporosis, degeneration of the intervertebral disc, etc.) on the flexibility of the spine can be investigated using this in-depth anatomically relevant approach.

The geometry of the majority of recently built 3D models of the spine has been derived from CT data [4], [6], [7], [9], [13], [14]. The main advantage lies in the fact that CT images provide very accurate and precise information on bone geometry [15]. In the majority of computational studies, e.g., [6]–[8], [10], [11], the global geometry of a FE model of a motion segment or of a multisegmental spine is based on the reconstruction of only one vertebra [7], due to the extremely complex vertebral geometry. Usually, the CAD or FE model of a given vertebra is copied and scaled to mimic the difference in size of each vertebra . The final FE model of the multisegmental spine is created by stacking the vertebrae on top of each other. The mean dimensions and shapes of additional spinal components, such as intervertebral discs, are defined according to the anatomical data provided in the literature and histological observations [7].

In contrast to many studies reported in the literature, the aim of this research is to create a patient specific complex 3D FE model of the thoracolumbar spine using commercial CAD/FE software and CT scans. The emphasis is placed on ensuring geometrical precision in the representation of the bone. In this context, the first main objective of the paper is to present the development of a model generation method. To this end, a robust, semi-automatic procedure for the generation of FE models directly from CT data is introduced. This procedure allows highly anatomically accurate FE representations of each vertebra in the thoracolumbar spine to be generated, using CT images of a specific thoracolumbar spine specimen. The second main objective of the paper is to present the results of a computational study, performed using the generated model, where loading conditions on the thoracolumbar spine are varied. This study demonstrates the capabilities of the model and also specifically demonstrates the sensitivity of the biomechanical behaviour of the thoracolumbar spine to variations in the applied loading conditions.

# 2. Reconstruction of the vertebrae

## 2.1. CT image processing

The generation of 3D FE models of bone from CT scans involves two main steps. These are geometry definition and the application of a specific meshing procedure. In order to generate an FE model of the bone structure, CT data has to be processed to extract the desired information such as bone geometry and tissue density.

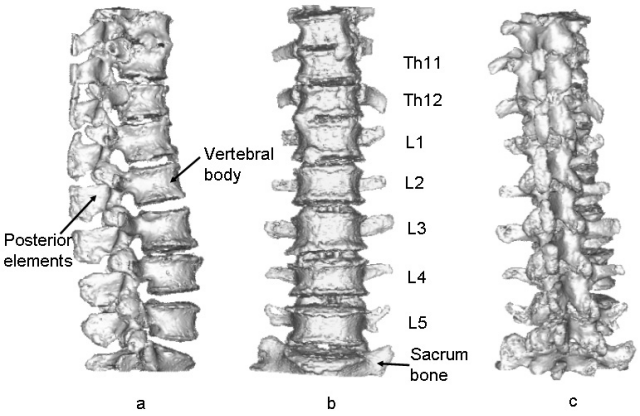


Fig. 1. 3D visualisation (MIMICS) of the thoracolumbar spine based on CT data obtained from Rice University: (a) side view, (b) front view, (c) back view. Vertebrae Th11–L5 are indicated

In this study, the geometry of each thoracolumbar component (Th11–L5) was derived from a series of CT scans from a 63 year old male cadaver (Figure 1). The medical images were obtained from Rice University, USA. The specialist software MIMICS (© 2004, Materialise NV) was used to process the medical images and derive the geometry. In order to define an accurate geometry of each vertebra in the thoracolumbar column, the bone tissue was segmented by thresholding and the pixels having grey values in the threshold range were treated as bone tissue and collected in a segmentation mask. The segmentation mask was automatically three dimensionally reconstructed using a region growing function available in MIMICS (Fig-

ure 1). This option allowed one to assess the quality of the segmentation mask and the visualisation of an entire bone structure directly from 2D CT images (Figure 1). One of the most important requirements which must be satisfied during image processing was that the segmentation mask had to make a closed volume. Thus, in many regions, it was necessary to edit the segmentation mask manually to make a closed volume, by including a single pixel or group of pixels to the segmentation mask.

After processing the CT images, two different modelling procedures, namely the CAD based method and the STL-CAD based method, were applied to define an accurate geometry for each vertebra in the seven-level thoracolumbar spine.

## 2.2. Surface representation of the thoracolumbar spine

### 2.2.1. CAD based approach

In the context of the present work, the CAD based approach can be defined as a process of model generation where emphasis is placed on preparation and manipulation of the bone geometry based on a series of contour lines and surfaces.

One of the many advantages of MIMICS software is that the MedCAD module allows one to generate the surface representation of a given object in a fully automated way. However, in the case of the spine, it was not possible to generate a single surface due to the extremely complex geometry of the vertebra.

In order to speed up the reconstruction process, the vertebral bodies and posterior elements (Figure 1) were modelled separately. This decision was based on the fact that the geometry of the vertebral body is simple relative to that of the bony ring and its surface representation could be generated easily in MIMICS. The vertebral bodies were separated from the posterior elements by deleting rows of pixels from each cross-sectional slice. The posterior elements themselves were then split into five separate segments to further reduce geometrical complexity. Following this, seven segmentation masks were applied: two for the vertebral body (cortical shell and trabecular core) and five for the posterior element segments. This is illustrated in Figure 2.

Following the image processing steps performed in MIMICS, sets of contour lines that bordered the specified bone tissue were determined for each slice, in order to transfer the reconstructed images of the lumbar spine into a CAD/FE environment.

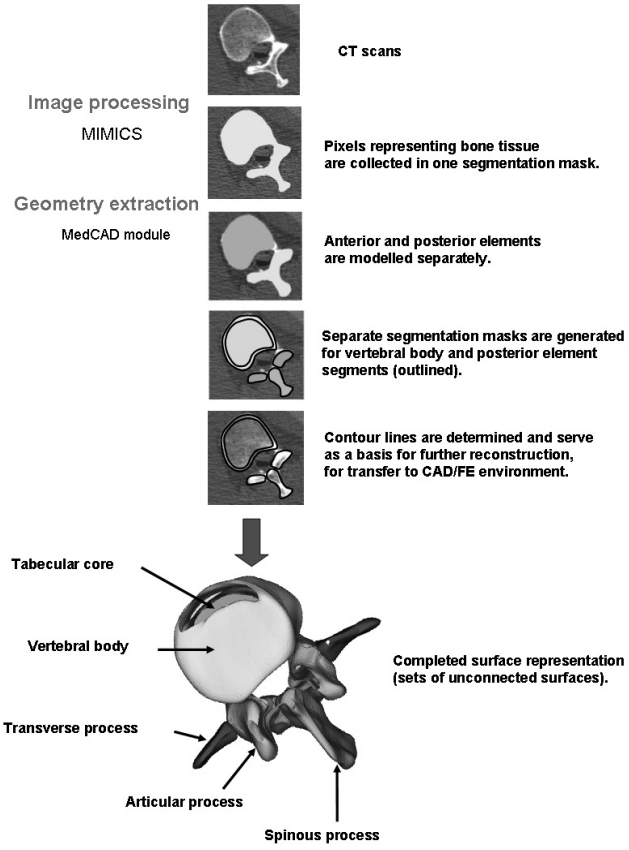


Fig. 2. Schematic representation of the CAD based method

#### 2.2.1.1. Vertebral body

For the vertebral body, the surface representation was generated using the MedCAD module via the CAD based method (Figure 2). A set of contours that bordered the external cortical shell and the inner trabecular core were automatically determined in each slice. These lines served as the basis for further construction of a geometrical model. In order to speed up the geometry definition process, a group of surfaces was fitted automatically to the newly generated contours. The vertebral bodies were represented by large smooth surfaces that bordered the cortical and trabecular bone.

#### 2.2.1.2. Posterior elements

The CAD based approach was initially used to model the posterior bony processes of the L5 vertebra using the steps illustrated in Figure 2. As mentioned above, the basic segmentation mask describing the posterior elements of the vertebra was divided into five distinct parts. This was done by deleting rows of pixels from each cross-sectional slice. Following this, a set of five unconnected segmentation masks was applied. Each mask represented a different process or group of processes in the bony ring: two for the trans-

verse processes, two for the articular processes and one for the spinous process (Figure 2). A group of surfaces that represented the different processes was then fitted automatically to the contour lines.

#### 2.2.1.3. Whole vertebra

The surface representation of the whole vertebra (vertebral body and posterior elements) was exported as an IGES file into the ANSYS (©2003, ANSYS Inc.) package. Using the Pre-Processor module in ANSYS each surface was divided into smaller segments in order to create new areas and to fill the gaps between the original adjacent surfaces. Once the surface sections for a given vertebra were completely joined together, the result was considered as a solid model of the vertebra. This was a labour intensive process, chiefly due to the geometrical complexity of the posterior elements.

### 2.2.2. STL-CAD based approach

The CAD based solid model generation procedure gave very good results but was rather time consuming (up to 100 hours to generate a solid model of the vertebrae) and was insufficiently robust to be relied upon exclusively for developing patient specific FE models of the thoracolumbar spine. Therefore, an alternative procedure was considered, that presented the possibility of a certain degree of automation. This alternative procedure was particularly useful for dealing with the bony processes.

The development of a faster and more robust geometry definition method evolved from Rapid Prototyping (RP) technology and the Stereolitography (STL) file format. In the STL file format a 3D object is represented by sets of triangles that form the outer shell of a volume, where the triangles share common sides and vertices.

In the context of the present work, the STL-CAD based method can be defined as a process of model generation where emphasis is placed on manipulation and modification of triangular STL geometrical mesh representations of an object, to convert it into a closed surface, resulting in a solid model.

### 2.2.3. CAD + STL-CAD combination

In the present work, the final solid models of the vertebrae were generated using a combination of the CAD and the STL-CAD approaches, with the CAD based method being used for the vertebral bodies and the STL-CAD based method being used for the geometrically complex posterior elements. The combined process is illustrated in Figure 3. For the posterior elements, an intact segmentation mask representing the whole of the posterior bony processes was generated in MIMICS and automatically converted into the STL format. The software module STL+ within MIMICS was used to generate the triangular mesh representation and to transfer it to HyperMesh (© 2004, Altair Engineering, Inc.) software as an STL file. The special "FE → Surf" panel in HyperMesh was used to automatically convert the irregular, triangular mesh representation of each bony ring into a closed surface that closely fitted the triangular surface mesh.

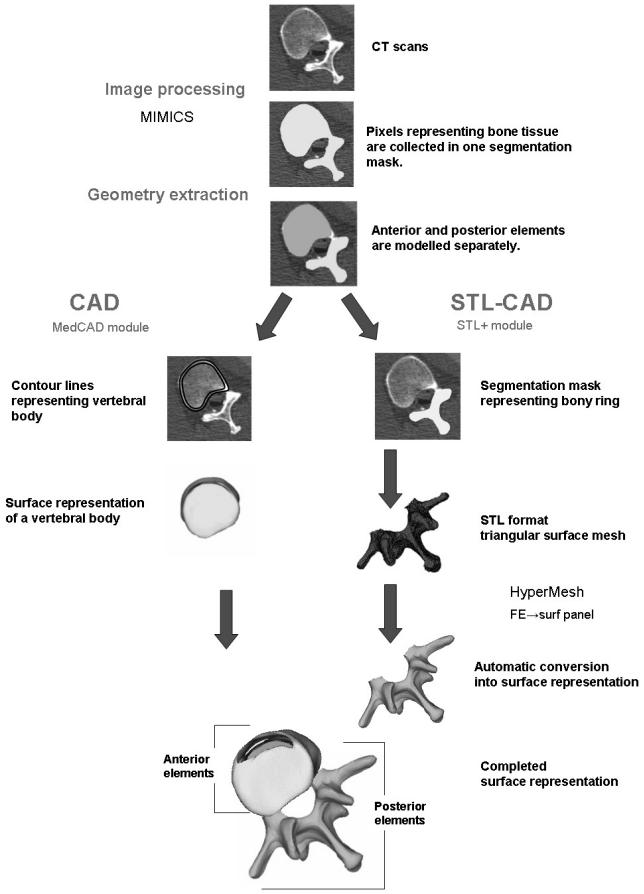


Fig. 3. Schematic representation of a combination of the CAD and STL-CAD based methods

In order to generate the complete solid model of the vertebra, the surface representation of the vertebral body generated using the CAD based method as described above and saved in IGES format was imported into HyperMesh. Using the geometry module in HyperMesh, the surfaces were manually corrected to smooth irregular areas and to join the vertebral body surface to the bony ring surface, resulting in a solid model of the vertebra. The final solid models for each of the T11–L5 vertebrae are shown in Figure 4.

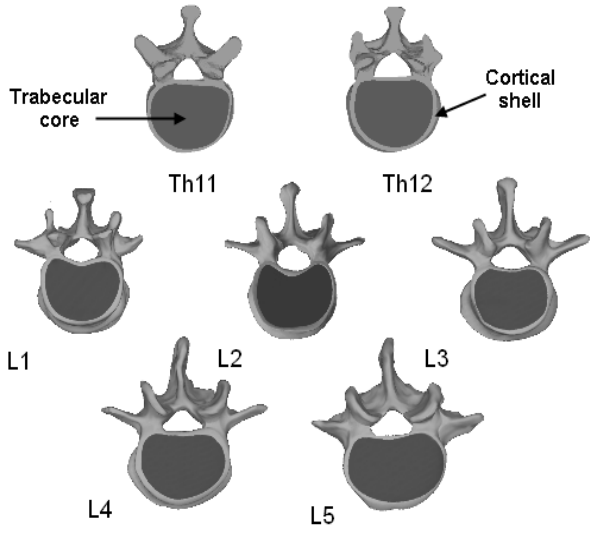


Fig. 4. Solid models of the seven anatomically different vertebrae

This combination of methods was found to be most appropriate for the vertebrae and the generation of the solid model of the single vertebrae was speeded up by a factor of ~5 in comparison to CAD based modelling alone. The CAD based method produced very accurate representations of the cortical tissue and trabecular core and was the most effective for dealing with the geometrically simple vertebral bodies, while the STL-CAD based method was faster and more effective for dealing with the bony processes, due to their extremely complex geometry.

# 3. Finite element model of the thoracolumbar spine

After geometry definition, the next step in generating a 3D FE model is the application of a specific meshing procedure. Several techniques for generating meshes for bone structures have been developed [16]–[23], however geometry based meshing is the most commonly reported technique in the literature.

In general, geometry based meshing in orthopaedic FE modelling can be defined as a process of mesh generation where emphasis is placed on manipulation of the surface/volume representation of bone geometry, to make it suitable for easy mesh construction, using conventional meshing techniques. The most popular are the mapped and free mesh methods available in most commercial finite element packages, e.g., ANSYS, ABAQUS CAE, PATRAN and HyperMesh.

## 3.1. Meshing procedure

In order to examine the biomechanics of the seven level thoracolumbar spine, a complex 3D non-linear FE model that included soft tissue such as intervertebral discs and spinal ligaments was created. The solid models of the seven anatomically different thoracolumbar vertebrae shown in Figure 4 were used to create the FE model. HyperMesh was used in FE mesh generation and the commercial code ABAQUS (© 2004, ABAQUS, Inc.) was used for solving boundary value problems with the mesh.

In order to create the spinal column, all seven vertebrae were stacked one on top of the other. As the entire geometry was derived from a series of CT images, the distances between the vertebral bodies and facet joints, and the anatomical spinal curvatures, were preserved. Using the geometry module in HyperMesh, additional spinal components such as soft tissues were modelled.

In order to fill spaces between adjacent vertebral bodies, six intervertebral discs were created. From CT data the exact internal structure of the disc was not known, so using data from the literature, it was assumed that the nucleus pulposus filled 45% of the total disc area in cross-section and that its position was more posterior than central [27]. The cartilage and bony end-plates were also included in the solid model of the thoracolumbar spine. The volume of each of the thoracolumbar vertebrae was split into two subvolumes, namely vertebral body and posterior bony ring, and these subvolumes were meshed separately.

### 3.1.1. Spinal column

The vertebral bodies and the intervertebral discs were meshed using the mapped mesh approach. 3D, isotropic, 8-noded solid/brick elements were used in the modelling of the cortical shell, trabecular core, bony and cartilaginous end-plates, and the annulus matrix of the intervertebral disc. The thickness of the cortical shell varied for each vertebral body and was set to range from 1.5 to 2 mm. These values were based on the CT scan measurements.

A combination of element types was used for the intervertebral discs (Figure 5a). The annulus fibrosus was defined by three radial layers and modelled as a composite material consisting of fibres embedded in a ground substance. For the fibres, 3D truss elements were aligned in layers to form a criss-cross pattern placed at an average angle of 40° to the horizontal plane of the disc. The nucleus pulposus was simulated as an incom-

pressible material and represented by 8-noded hybrid solid elements with a low Young's modulus and a Poisson's ratio close to 0.5 [5], [25]. The ground substance of the annulus fibrosus (the annulus matrix) was represented by 8-noded solid/brick elements.

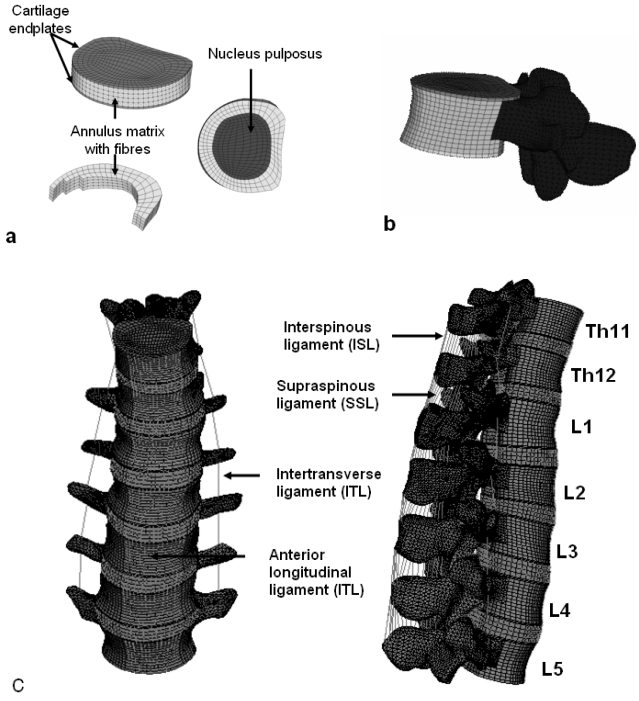


Fig. 5. Mesh of typical vertebra (a), structure of intervertebral disc (b), and complete model with three different views shown (c). Some of the spinal ligaments included in the model are also shown in (c)

### 3.1.2. Posterior processes

Due to the extremely complex geometry of the posterior part of the lumbar vertebrae, it was difficult to mesh the bony rings using the mapped mesh approach. Therefore, in order to speed up the meshing process and preserve the detailed geometry of the posterior spinal components, a different approach was considered. Instead of the 8-noded brick elements, 4-noded tetrahedral elements were used (Figure 5b). Combining tetrahedral elements with brick elements speeded up the entire meshing process for the vertebrae, relative to the previously considered methods. Moreover, the tetrahedral elements were able to give very accurate rendition of the bony ring surface geometry (Figure 5b). However, with this approach, only first order elements could be used to preserve the compatibility between the tetrahedral and brick elements. In the case of second order elements, the tetrahedral mesh (middle node) would not match up the higher order brick elements.

A preliminary FE analysis was carried out to study the effects of the mesh density and the combination of the different element types on the stress distribution. To analyse the effect of mesh density, a single motion segment (L4L5) was considered and a bending moment of 7.5 Nm was applied. The results from the mesh shown in Figure 5b were compared to those produced by a mesh that was approximately three times as dense. There was no appreciable difference in the stress distributions, leading to the conclusion that the mesh shown in Figure 5b was sufficiently accurate. To investigate the combination of the brick and tetrahedral elements, a single vertebra was subjected to a compressive load along the spinal column direction. The results clearly showed that the combination of elements did not produce discontinuities in stress distribution; a smooth stress transition between the vertebral body and the posterior processes was observed.

### 3.1.3. Facet joints

The facet joints were modelled as a 3D frictionless contact problem using interface GAP elements to simulate the contact between the articulating faces. The articulating faces were represented by series of convex and concave surfaces. The initial gap between the two facet surfaces was based on the CT scan measurements and was about 0.8 mm. An average of 25 GAP elements were used to model each facet joint contact.

### 3.1.4. Spinal ligaments

Seven spinal ligaments, namely the anterior longitudinal ligament, posterior longitudinal ligament, ligamentum flavum, intertransverse ligament, capsular ligament, interspinous ligament and supraspinous ligament were considered in the model (Figure 5c ). In order to mimic anatomical observations, the points of ligament attachment to the bone were chosen from anatomy textbooks [26]–[28]. The spinal ligaments were modelled using two different elements, namely non-linear springs and truss elements. It has been reported in the literature [24] that the ligamentum flavum and anterior and posterior longitudinal ligaments have a pre-tension in the neutral position of the spine. Based on data from the literature [24], the initial pre-tension values for non-linear spring elements (ABAQUS-SPRINGA) representing these ligaments were calculated, and were set to 14 N, 2 N and 1.5 N for the ligamentum flavum, anterior longitudinal and posterior longitudinal ligaments, respectively.

On the basis of the physical properties of spinal ligaments in general [24], 3D truss elements (ABAQUS-T3D2) were chosen to simulate the remaining four liga-

Table 1. Material properties and material specifications for the bony parts of the spine and the intervertebral discs

| Component | Elements | | Material properties [5], [6], [13], [41] | |
|---|---|---|---|---|
| | Type | Number | *E*(MPa) | ν |
| Bony endplate | 8-noded brick | 384 | 1000 | 0.3 |
| Cortical shell | 8-noded brick | 672 | 12000 | 0.3 |
| Trabecular core | 8-noded brick | 3936 | 344 | 0.2 |
| Bony ring | 4-noded tetra | 17242–33226 | 3500 | 0.3 |
| Cartilage endplate | 8-noded brick | 384 | 24 | 0.4 |
| Nucleus | 8-noded brick | 864 | 1.0 | 0.499 |
| Annulus matrix | 8-noded brick | 672 | 4.2 | 0.45 |
| Fibres | 2-noded truss | 448 | 500 | 0.3 |

Table 2. Material properties and element specification for the spinal ligaments

| | Element | | Area | Material properties [3], [5], [6], [10], [11], [13], [41] | |
|---|---|---|---|---|---|
| | Type | Number | mm$^2$ | *E* (MPa) | ν |
| ALL | SPRINGA | 1032 | Non-linear force-deflection response determined from [27] | | |
| PLL | SPRINGA | 258 | | | |
| LF | SPRINGA | 9 | | | |
| ITL | T3D2 | 1 | 5.0 | 54.4 | 0.3 |
| CL | T3D2 | 26 | 48.4 | 24.4 | 0.3 |
| ISL | T3D2 | 12 | 42.7 | 16.9 | 0.3 |
| SSL | T3D2 | 150 | 38.9 | 34.1 | 0.3 |

(ALL) anterior longitudinal ligament, (PLL) posterior longitudinal ligament, (LF) ligamentum flavum, (ITL) intertransverse ligament, (CL) capsular ligament, (ISL) interspinous ligament, (SSL) supraspinous ligament.

ments. This decision was based on the fact that this type of element could be used in 3D to model slender, line-like structures that support loading only along the axis or the centreline of the element [29]. The completed FE model of the thoracolumbar spine consists of 211 035 elements and 86 875 nodes (Figure 5c).

The assignment of material properties for all bony spinal components and intervertebral discs was based on literature studies [3], [5]–[7], [30] and the different materials were assumed to be linear, homogeneous and isotropic (Table 1). All the physical and material properties of the spinal ligaments were also derived from the literature [6], [24], [31] and are given in Table 2.

# 4. Effect of the various loading conditions on the behaviour of the thoracolumbar spine

The FE model was employed in the series of loading simulations described below. The purpose of the simulations was to demonstrate the capabilities and uses of the model in illustrating the biomechanical behaviour of the thoracolumbar spine and also to demonstrate the sensitivity of this behaviour to variations in the applied loading conditions. The FE model of the thoracolumbar spine was subjected to axial compression (along the *Z*-axis shown in Figure 6) and loaded to 1000 N. This static load simulated standing or walking situation for a person with a weight of 70 kg [24]. Given that high local strains and stresses were expected in the simulations, large strain kinematics were assumed using the NLGEOM keyword in ABAQUS. Three specific loading conditions were considered. In the first model (LC1), the load was applied to a rigid plate located on the top of the first vertebra (Th11) in the spinal column (Figure 6a). The model was rigidly fixed on the bottom and all nodes attached to the end-plate of the L5 vertebra were restrained in all directions. In addition, to model support from the sacrum bone at the base of the spine the nodes on the surface of the lower facet joints of L5 vertebrae were also restrained.

The load acting on the spine is shared between the intervertebral discs and facet joints and this

distribution varies depending on the spinal posture. In a normal healthy spinal unit, the disc is the major anterior load bearing structure. It has been reported in the literature that the facet joints can carry 3 to 25% of total loading, and this could increase up to 47% if the facet joint is arthritic [24]. Therefore, in the second model (LC2), the 1000 N was applied along the *Z*-axis to the upper vertebral body and to the facet joint of the Th11 vertebrae (Figure 6b). In this case, the compressive force was divided: 75% acted on the upper vertebral body and 25% acted on the facet joint.

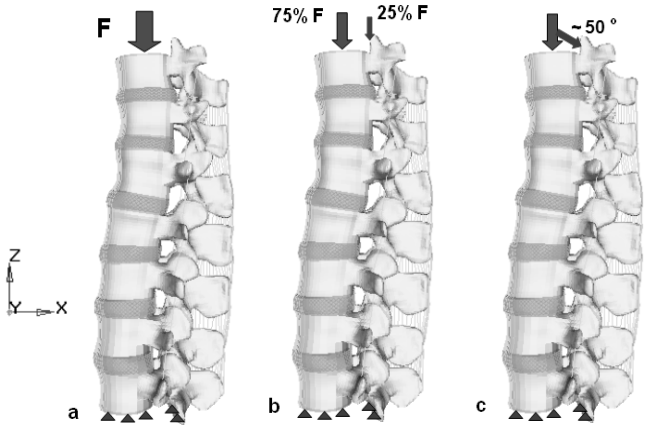


Fig. 6. Loading conditions assumed in three FE models of the thoracolumbar spine: LC1 (a), LC2 (b), and LC3 (c). All models were restrained at the bottom and inferior articular processes of the L5 vertebrae

The third model (LC3) was similar to LC2 model and 75% of the axial compressive load was applied along the *Z*-axis to the top of Th11 vertebrae (Figure 6c). It has been reported in the literature that the orientation of the facet joints depends on the specific region of the spine and also varies between different individuals [24]. Typically, in the thoracic region, the facet joints are oriented at an angle to the vertical direction, whereas the orientation of the lumbar facet joints is almost parallel to the vertical direction. Therefore, to mimic the interaction between facet joints of thoracolumbar spine, in the LC3 model, the 25% of the total loading was applied to the facet joints at an angle of approximately 50° to the *Z*-axis.

## 4.1. Results

The effect of the compressive load on the changes in compressive stiffness and stress distribution within the thoracolumbar spine was investigated.

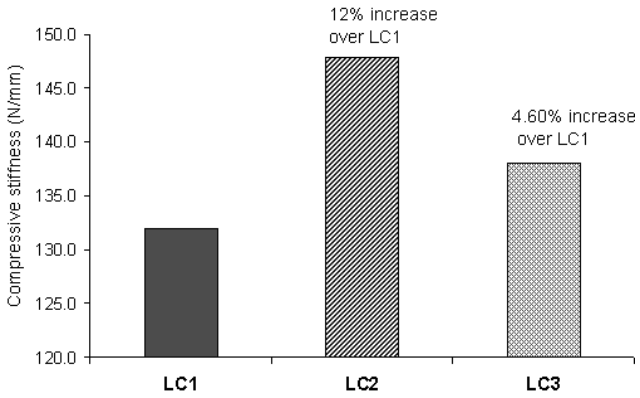


Fig. 7. Changes in the compressive stiffness calculated for all three FE models. The highest difference between results was found between the LC1 and LC2 cases

### 4.1.1. Compressive stiffness

The apparent compressive stiffness of the FE models was calculated by dividing the axial compressive load of 1000 N by the maximum vertical displacement measured at the point located on the top of the thoracolumbar column. In order to determine the effect of the three boundary conditions on the compressive stiffness of the spine, the results obtained from LC2 and LC3 were compared with those of the first loading case (LC1). The results showed that the apparent compressive stiffness of the thoracolumbar spine depended on the assumed loading conditions (Figure 7). The lowest compressive stiffness was noticed when the external load of 1000 N was applied only to the top of the spinal column. By sharing the compressive load between the spinal column (75%) and bony processes (25%) an increase in the compressive stiffness was produced: 12% more than LC1 for the LC3 case and 4.6% more than LC1 for the LC3 case. Clearly, moving the load in the posterior direction significantly increased the apparent compressive stiffness of the spine. This makes sense when one considers that load transfer down the anterior part of the spine involves load transfer through the intervertebral discs (that are relatively compliant). Moving the load in the posterior direction means that a greater proportion of the load is carried by the posterior elements through the facet joints (that are stiff relative to the intervertebral discs).

### 4.1.2. Stress distribution

The von Mises stress distributions for all the FE models of the thoracolumbar spine are shown in Figures 8–10. As is clear from Figure 8, the vertebral bodies were most highly stressed in the upper mid section of the thoracolumbar spine, in particular for L1. This is an

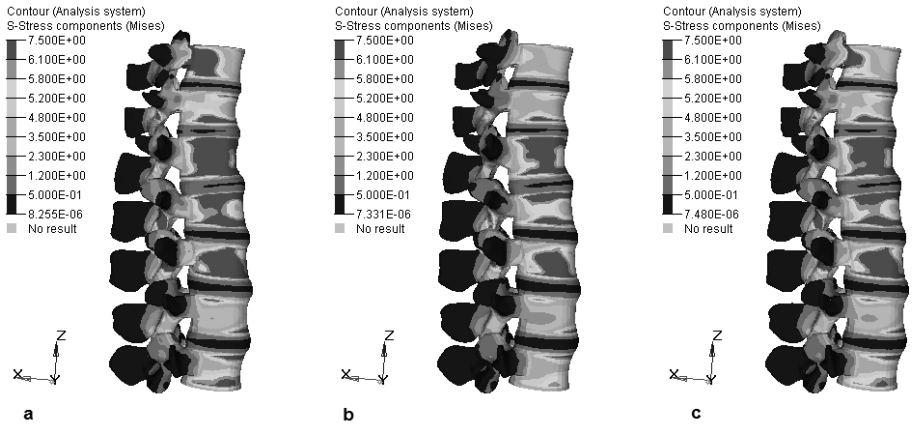


Fig. 8. The overall von Mises stress (MPa) distribution in the three FE models of the thoracolumbar spine under the compressive load of 1000 N: LC1 (a), LC2 (b), and LC3 (c) load cases

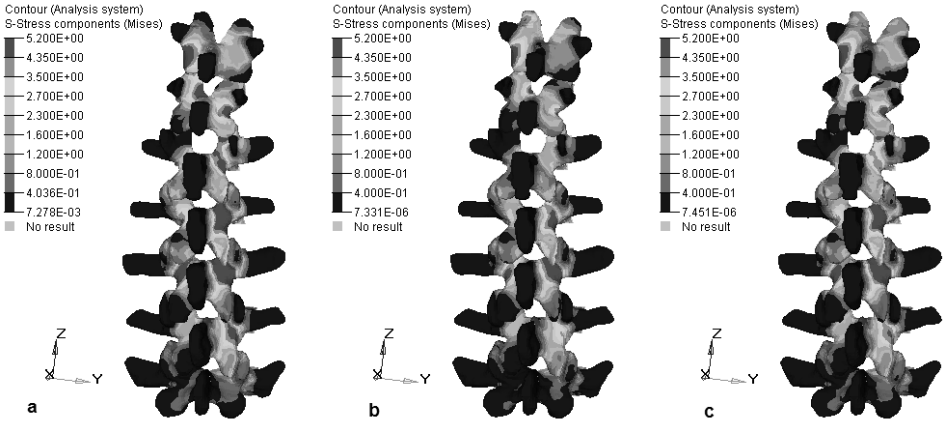


Fig. 9. The von Mises stress (MPa) distribution in the posterior bony rings for: LC1 (a), LC2 (b), and LC3 (c) load cases

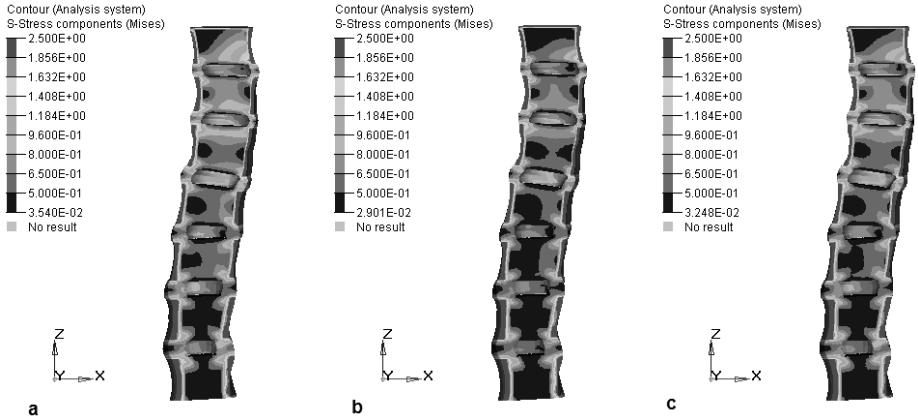


Fig. 10. The von Mises stress distribution (MPa) within the spinal column of the thoracolumbar spine (cross-section in *X*–*Z* plane) for the three FE models with different loading conditions: LC1 (a), LC2 (b), and LC3 (c)

interesting result and it could be concluded that this region of the thoracolumbar spine carries the highest risk of injury (fracture). This is in good agreement with the clinical observations reported in the literature [32], [33]. As regards load case dependence, the highest vertebral body stresses were observed for LC1 (maximum stress values ranged from 5.8 to 10.5 MPa), followed by LC3 (maximum stress values ranged from 5.8 to 8.2 MPa),

with the lowest stresses observed for LC2 (maximum stress values ranged from 4.3 to 7.4 MPa). This is consistent with the shift in the applied load in the posterior direction, reducing the vertebral body loading, and also the lower changes in spinal curvature under load for the LC2 case.

Stresses in the posterior elements are shown in Figure 9. High stresses were observed close to the facet joints. Across the three loading cases the most highly stressed facet joints were for the Th11–Th12 and the L2–L3 vertebrae.

Finally, the overall stress distributions within the vertebral bodies were examined for the three loading cases (Figure 10). The results showed that the trabecular cores experienced much lower stresses than the cortical shells. However, the largest areas with high stresses in the trabecular cores were still observed in the upper part of thoracolumbar spine (Th12–L2), which correlates with the observations for cortical shell stresses (Figure 8). In these regions, stress magnitudes between 1.2 and 1.5 MPa were observed for the LC1 and LC3 load cases (Figure 9a, c) and lower stress magnitudes of 0.8 to 1.2 MPa were observed for the LC2 load case. For all vertebrae, the lowest stress values were observed in the central (midtransverse) part of the trabecular core. This was in agreement with observations reported in the literature that the contribution of trabecular bone to the total load carrying function of the vertebral body depends on its location within the vertebral body [5], [34], [35].

Another interesting observation is the difference between the LC2 and LC3 load case results; clearly the LC2 load case, where the posterior part of the load was applied vertically, had a more significant effect on the results, relative to the LC1 load case, than the LC3 load case, where the posterior part of the load was applied at an angle. This could be related to the fact that in applying the load at an angle the vertical component of the load was lowered. One final overall observation is significant lack of symmetry in the stress distributions between the right side and the left side of the spine, which could be attributed to the curvature of this specific spinal specimen.

## 5. Summary and conclusions

The model building strategy to identify an efficient and robust finite element model generation method for the complex spine system has been presented. Two different modelling procedures were considered: CAD based and STL-CAD based. In the authors' opinion, the CAD based method produced very accurate representations, but was time consuming and required a lot of manual effort for complex geometries. The STL-CAD approach was a faster and more robust approach for dealing with very complex geometries. Based on the extensive model generation work performed in this research, it is concluded that for anatomical structures such as the vertebra, which consist of simple and complex geometry regions, the optimum method for solid model generation involves the combination of these two approaches. In addition, the entire meshing procedure for the vertebrae was significantly speeded up by combining 3D tetrahedral elements with brick elements, relative to conventional mapped mesh generation procedures. The resulting model generation method allowed for flexibility in element choice and in element type combinations. The computational results presented here clearly indicated that the combination of 3D tetrahedral and brick elements did not produce discontinuities in stress distribution. A smooth stress distribution between the vertebral bodies and anterior processes was observed.

The combination of two modelling and meshing approaches allowed the creation of a patient specific 3D FE model of the thoracolumbar spine. In contrast to many studies [7], [11], [36], [37] where the global geometry of the lumbar spine was derived from CT scan based reconstructions of only one vertebra, here seven detailed 3D CAD solid models of the anatomically different Th11–L5 vertebrae were created.

The FE model was subjected to various compressive loads to assess the overall behaviour of the thoracolumbar spine. The purpose of this case study was to illustrate the usefulness of the model in illustrating the mechanical behaviour of the spine and also to demonstrate the sensitivity of this behaviour to variations in the applied loading conditions. In general, the results showed that the model was capable of giving very detailed quantitative information on the mechanical behaviour of the spine, and as such could be considered to be a very useful spinal analysis tool. In specific terms, for example, there was a significant lack of symmetry between the left and right side stress levels. Such issues are of clinical relevance; in particular the locations of high stress indicated sites where fracture or degenerative changes are likely to occur. Indeed, the predicted locations of the most highly stressed vertebral bodies correlate well with clinical data on locations of spinal fracture [32], [33].

The results clearly showed that the specific loading conditions applied in the computational study had a strong impact on the stress patterns of the spine. Even though the load cases were restricted almost

exclusively to axial compressive loading, the movement of part of the load from the anterior (vertebral body) to the posterior elements resulted in a significant increase in apparent compressive stiffness (12%) and caused changes in stress levels. It was also observed that these effects seem to have been weaker for the case where the posterior load was applied at an angle. One main conclusion from this is that the model predicts that the biomechanical response of the spine is very sensitive to relatively small changes in the loading condition. Once again, this has important clinical implications, for example, in terms of the relationship between bodily posture and the risk of spinal damage.

Due to fact that FE models are mathematical approximations of reality they require through experimental validation. In a follow-on article, the performance of the model presented in this paper is assessed relative to experimental mechanical test data for an equivalent thoracolumbar spine.

In the authors' opinion, models, such as the one presented in this study, are important tools in computational spine research and clinical studies. First of all, a FE allows one to create a variety of models that can be examined under different physiological loading conditions. Moreover, computational simulations provide information that cannot be easily obtained from experimental studies, such as the stress distribution within the vertebrae and intervertebral discs. Looking to the future, the model generated in this study, could serve as valuable tool for spinal implant design, as the detailed effects of an implant on the biomechanical response of a specific spine could be examined in a "pre-clinical" setting.

## Acknowledgements

The authors acknowledge support from the Programme for Research in Third Level Institutions (PRTLI), administered by the Higher Education Authority (HEA), and the Irish Council for Science, Engineering and Technology (IRCSET). The authors would like to thank Prof. Michael Liebschner and Mr. Wafa Tawackoli from Rice University, Texas, USA, for providing CT scan data. The finite element simulations in the work were performed on the SGI 3800 and SGI Altix high performance computers at NUI, Galway.

## References

[1] SHIRAZI-ADL A., PARNIANPOUR M., *Computer techniques and computational methods in biomechanics*, [in:] *Biomechanical Systems Techniques and Applications*, C. Leondes (ed.), CRC Press LLC, 2001, pp. 1–1:1–36.

[2] FAGAN M.J., JULIAN S., MOHSEN A.M., *Finite element analysis in spine research*, Journal of Engineering in Medicine, 2002, 216, (Part H), pp. 281–298.

[3] NABHANI F., WAKE M., *Computer modelling and stress analysis of the lumbar spine*, Journal of Materials Processing Technology, 2002, 127, pp. 40–47.

[4] LIEBSCHNER M., KOPPERDAHL D.L., ROSENBERG W.S., KEAVENY T.M., *Finite element modelling of human thoracolumbar spine*, Spine, 2003, 28, (6), pp. 559–565.

[5] POLIKEIT A., *Finite element analyses of the lumbar spine: Clinical applications*, [in:] Faculty of Medicine, Experimental Biomechanics, 2002, University of Bern, Bern.

[6] PITZEN T., GEISLER F., MATTHIS D., MULLER-STORZ H., BARBIER D., STEUDEL W.I., FELDGES A., *A finite element model for predicting the biomechanical behaviour of the human lumbar spine*, Control Engineering Practice, 2002, 10(1), pp. 83–90.

[7] NAOAILLY J., LACROIX D., PLANELL J., *The mechanical significance of the lumbar spine components – a finite element stress analysis*, [in:] 2003 Summer Bioengineering Conference, 2003, Sonesta Beach Resort in Key Biscayne, Florida.

[8] ZANDER T., ROHLMANN A., CALISSE J., BERGMANN G., *Estimation of muscle forces in the lumbar spine during upper-body inclination*, Clinical Biomechanics, 2001, 16 Supplement, pp. S73–S80.

[9] EBERLEIN R., HOLZAPFEL G.A., FROHLICH M., *Multi-segment FEA of the human lumbar spine including the heterogenity of the annulus fibrosus*, Computational Mechanics, 2004.

[10] SHIRAZI-ADL A., *Biomechanic of the lumbar spine in sagittal/lateral moments*, Spine, 1994, 19, pp. 2407–2414.

[11] EZQUERRO F., SIMON A., PRADO M., PEREZ A., *Combination of finite element modeling and optimization for the study of lumbar spine biomechanics considering the 3D thorax-pelvis orientation*, Medical Engineering and Physics, 2004, 26(1), pp. 11–22.

[12] SHIRAZI-ADL A., PARNIANPOUR M., *Load-bearing and stress analysis of the human spine under a novel wrapping compression loading*, Clinical Biomechanics, 2000, 15(10), pp. 718–725.

[13] PINTAR F.A., YOGANANDAN N., MYERS T.J., ELHAGEDIAB A., SANCES A., *Biomechanical properties of human lumbar spine ligaments*, Journal of Biomechanics, 1992, 25(11), pp. 1351–1356.

[14] POLIKEIT A., FERGUSON S.J., NOLTE L.P., ORR T.E., *Factors influencing stresses in the lumbar spine after the insertion of intervertebral cages: finite element analysis*, European Spine Journal, 2003, 12(4), pp. 413–420.

[15] TALEB-AHMED A., DUBOIS P., DUQUENOY E., *Analysis methods of CT-scan images for the characterization of the bone texture: First results*, Pattern Recognition Letters, 2003, 24, pp. 1971–1982.

[16] CANTON B., GILCHRIST M., *It's all in head*, IEI, 2003, pp. 45–47.

[17] CAMACHO D.L.A., HOPPER R.H., LIN G.M., MYERS B.S., *An improved method for finite element mesh generation of geometrically complex structures with application to the skullbase*, Journal of Biomechanics, 1997, 30(10), pp. 1067–1070.

[18] CARRIGAN S.D., WHITESIDE R.A., PICHORA D.R., SMALL C.F., *Development of a three-dimensional finite element model for carpal load transmission in static neutral posture*, Annals of Biomedical Engineering, 2003, 31, pp. 718–725.

[19] COUTEAU B., PAYAN Y., LAVALLEE S., *The mesh-matching algorithm: an automatic 3D mesh generator for finite element structure*, Journal of Biomechanics, 2000, 33(7), pp. 1005–1009.

[20] KEYAK J.H., MEAGHER J.M., SKINNER H.B., C.D.M. Jr., *Automated three-dimensional finite element modelling of bone: a new method*, Journal of Biomedical Engineering, Sept. 1990, 12, pp. 389–397.

[21] LENGSFELD M., SCHMITT J., ALTER P., KAMINSKY J., LEPPEK R., *Comparison of geometry-based and CT voxel-based finite element modelling and experimental validation*, Medical Engineering and Physics, 1998, 20(7), pp. 515–522.

[22] WIRTZ D.C., PANDORF T., PORTHEINE F., RADERMACHER K., SCHIFFERS N., PRESHER A., WEICHERT D., NIETHARD F.U., *Concept and development of an orthotropic FE model of the proximal femur*, Journal of Biomechanics, 2003, 36, pp. 289–293.

[23] VICECONTI M., BELLINGERI L., CRISTOFOLINI L., TONI A., *A comparative study on different methods of automatic mesh generation of human femurs*, Medical Engineering and Physics, 1998, 20, pp. 1–10.

[24] WHITE A.A., PANJABI M., *Clinical biomechanics of the spine*, Philadelphia: J.B. Lippincott Company, 1990.

[25] POLIKEIT A., NOLTE L.P., FERGUSON S.J., *Simulated influence of osteoporosis and disc degeneration on the load transfer in a lumbar functional spinal unit*, Journal of Biomechanics, 2004, 37(7), pp. 1061–1069.

[26] GRAY H., *Anatomy of the Human Body*, 2000: Bartleby.com.

[27] LARSEN W., *Anatomy*: *Development, Function, Clinical Correlations*, ed. Saunders, 2002, Philadelphia, Pennsylvania, Elsevier Science (USA), 741.

[28] AGUR A.M.R., LEE M.J., *Grant's atlas of anatomy*, Philadelphia, Lippincott Williams and Wilkins, 1999.

[29] ABAQUS/STANDARD, ed. USER MANUAL version 6.4. Vol. II. 2003.

[30] CHOSA E., TOTORIBE K., TAJIMA N., *A biomechanical study of lumbar spondylolysis based on a three-dimensional finite element method*, Journal of Orthopaedic Research, 2004, 22(1), pp. 158–163.

[31] HEIDARI B., NAJARIAN S., *Prediction of load sharing among lumbar spine, using finite element approach*, [in:] 12th Conference of the European Society of Biomechanics, Dublin, 2000.

[32] FERGUSON S.J., STEFFEN T., *Biomechanics of the aging spine*, European Spine Journal, 2003, 12, (Suppl. 2), pp. S97–S103.

[33] SLOANE P.A., MCCABE J.P., *A demographic analysis of traumatic spinal injury in the West of Ireland from August to October 2000*, [in:] 28th Sir Peter Freyer Memorial Lecture and Surgical Symposium in Association with the Irish of Surgical Oncology, Galway, Ireland, 2003.

[34] HOMMINGA J., *Osteoporosis changes the amount of vertebral trabecular bone at risk of fracture but not the vertebral load distribution*, Spine, 2001, 26(14), pp. 1555–1561.

[35] SILVA M., KEAVENY T.M., HAYES W.C., *Load sharing between the shell and centrum in the lumbar vertebral body*, Spine, 1997, 22(2), pp. 140–150.

[36] LEE K.K., TEO E.C., *Effects of laminectomy and facetectomy on the stability of the lumbar motion segment*, Medical Engineering and Physics, 2004, 26(3), pp. 183–192.

[37] ZANDER T., ROHLMANN A., BERGMANN G., *Influence of ligament stiffness on the mechanical behavior of a functional spinal unit*, Journal of Biomechanics, 2004, 37(7), pp. 1107–1111.